Actively mode-locked and Q-controlled Nd:glass laser

I. V. Tomov,[a] R. Fedosejevs,[b] and M. C. Richardson

National Research Council of Canada, Division of Physics, Ottawa K1A OR6, Canada

(Received 28 August 1978; in final form, 20 September 1978)

A Q-controlled Nd:glass ring laser system has been developed which is actively mode-locked by means of either KD*P or $LiNbO_3$ electro-optic modulators and is capable of producing 1.5 mJ, 100 ps, 1.06 μm pulses synchronized to better than 400 ps to an external event. By using prelase methods or saturable absorbers shorter pulses from 37 to 15 ps duration can be generated with poorer synchronization.

INTRODUCTION

For over a decade it has been possible to generate picosecond optical pulses using a variety of different laser systems.[1,2] There are many applications today which require well-characterized ultrashort light pulses. In addition, in some cases precise synchronization of such light pulses with arbitrary external events is desirable. These applications encompass many areas of physics, nonlinear optics, ultrafast photography, photochemistry, and photobiology, and the availability of such laser sources has been instrumental in the development of fields such as real-time reaction kinetic studies and laser-fusion. In particular an oscillator for present day laser fusion systems should produce well profiled pulses in the millijoule range whose energy and duration can be tailored to match the requirements of a particular investigation.[3,4] Since such systems commonly utilize pulses >100 ps, a separate oscillator is needed to produce synchronized ultrashort diagnostic probe pulses at a wavelength nonharmonically related to the main laser pulse. Our present studies were motivated by the necessity of producing a synchronizable optical probe pulse for use in diagnosing the plasma produced by a short, powerful, 1-ns CO_2 laser pulse.[5] A visible laser pulse has the inherent capability to probe plasma densities well beyond the critical density for 10.6-μm CO_2 laser radiation and thus is an ideal illumination source for shadowgraphy, Schlieren photography, interferometry, and other optical diagnostics of the plasma. However, the desire to utilize picosecond pulses for such applications with the consequential demands of certainty on pulse duration, amplitude and synchronizability, has emphasized the shortcomings of existing methods of short pulse generation and recently has stimulated considerable development of more reliable and controllable systems.

To date, the most common approach to the generation of intense short pulses has been by means of mode-locking techniques using saturable absorbers.[1,2] However studies of such mode-locked lasers have shown that the output radiation is statistical in nature and that the important parameters of pulse height, pulse duration, and interpulse background level fluctuate from shot to shot.[6-8] In addition, the statistical nature of the bleaching of the dye results in a variation in the time of appearance of the pulse train much greater than the train duration itself, making impossible its synchronisation to an external event.

An alternative technique for the production of short pulses, widely investigated theoretically and experimentally with cw lasers, utilizes active mode-locking of the laser resonator.[9-11] This approach leads to the generation of pulses of much weaker intensity but good reproducibility. However, in contrast, the incorporation of active mode-locking with Q-switched lasers has only recently received attention.[12-18] This technique has the advantage of producing pulses 3–4 orders of magnitude more intense than non-Q-switched devices, but, the incorporation of a normal fast Q-switch results in a pulse build-up time too short to allow effective pulse shortening. To circumvent these limitations we have developed a Nd : glass laser system in which the pulse formation and growth are controlled by means of active modulation and Q-control of the laser resonator. Some characteristics of this system have been reported previously.[15-17] Not only has this system proved useful in interferometry of CO_2 laser produced plasmas[19] but also it has found application in making gain and saturation measurements on a XeF excimer laser system.[20] The present paper outlines a detailed description of this Nd : glass laser system and its performance under a wide range of operation conditions.

I. LASER SYSTEM

A. Ring resonator

The laser system utilized a 2.5-m-long ring resonator formed by four prisms as shown in Fig. 1. The use of such a resonator allows easy positioning of the modulator and other optical elements at any point within the resonator. In addition it permitted the introduction of optical dispersion within the resonator through the use of dispersive prisms, and also it facilitated unidirectional travelling wave operation. Its principal disadvantage rested in the greater degree of alignment demanded as compared to an equivalent linear cavity.

The four prisms used were Pellin Brocca or Abbé prisms made from BK-7 glass giving 90° deviation of the beam with Brewster-angled entrance and exit windows. To obtain Brewster-angled propagation through the

 0034-6748/79/010009-08$00.60

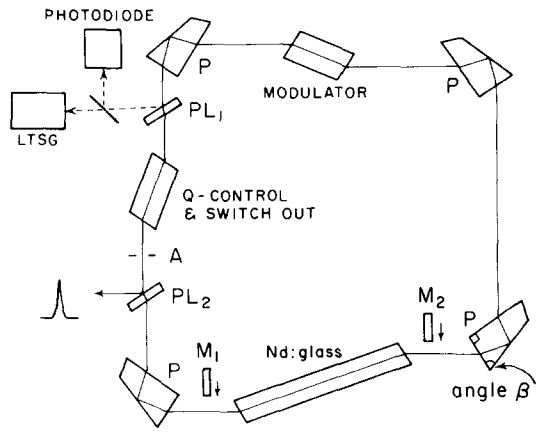

FIG. 1. Schematic of the Nd:glass ring laser system. A—aperture; LTSG—laser-triggered spark gap; M_1, M_2—1.06-μm dielectric mirrors; P—Pellin Brocca prisms; PL_1, PL_2—dielectric polarizers.

prism the angle β must be (135° − arctan$n$), where n is the index of refraction of the prism at the operating wavelength. In addition the prisms were mounted to give zero displacement of the beam as they were rotated.[21,22] The overall dispersion of the cavity depends on the relative orientation of the prisms.[23] In the case where all four prisms are orientated to give additive dispersion the single round trip bandwidth is

$$\Delta\lambda = \Delta\delta\left(\frac{8dn}{d\lambda}\right)^{-1},$$

where $\Delta\delta$ is the beam divergence, and $dn/d\lambda$ is the dispersion of the prism material. In the present laser cavity where $dn/d\lambda \simeq 1.6 \times 10^{-5}$ nm^{-1} and the beam divergence $\Delta\delta \simeq 0.3$ mrad, a single pass bandwidth of 2.3 nm was possible. Experience with dye ring lasers[23,24] has shown the laser output bandwidth is approximately 5 to 10 times narrower than the single pass bandwidth. Thus bandwidths limited to 0.25–0.5 nm should be possible in such a system. In the present laser system only a nondispersive orientation of the prisms has been used.

The alignment of the ring resonator was undertaken with considerable care. In practice it was found that the prisms had to be correctly aligned to within $\sim\pm0.05$ mrad for optimum laser output. The method employed consisted of forming a linear resonator around the glass rod using 50% and 100% reflectors on plane parallel substrates (mirrors M_1, and M_2, in Fig. 1). The output of this linear cavity was aligned through the ring resonator to reflect from the rear surface of the 100% reflector at the same spot as the laser radiation in the linear cavity. The alignment of the ring resonator was then adjusted so that the reflected beam propagated back through the resonator along the same path. The plane parallel mirror substrates could then be removed from the cavity and the resonator remained aligned for pulses propagating along the same path. As long as the temperature of the laser system was maintained within ±1 K it was found that the alignment procedure would not have to be repeated unless a change was made in the laser cavity elements.

B. Active modulator

Active mode-locking of a Q-switched laser system with a high depth of modulation can be accomplished using either an acousto-optic modulator or an electro-optic modulator. An acousto-optic mode-locker is easier to implement and requires only 20 to 50 W of rf driver power to operate. Unfortunately there are limitations to such a mode-locker. For high depth of modulation, operation is restricted to the individual acoustic resonant frequencies of the device. In addition the maximum depth of modulation is limited by heating of the modulator block during the modulation pulse. The amplitude transmission function $f(t)$ of such a modulator can be defined as

$$f(t) = \cos(\theta_m \sin 2\pi f_m t), \tag{1}$$

where f_m is the modulation frequency, and θ_m is the modulation parameter describing the depth of modulation.[14,17] For acousto-optic modulators this modulation parameter depends on the acoustic efficiency of the modulator and the rf drive power available. The highest acoustic modulation parameter obtained to date in a high power laser system at 1.06 μm is $\theta_m = 1.48$.[4]

For the present system a high modulation parameter and continuous frequency tunability was desirable in order to synchronize to another mode-locked laser system. Thus, an electro-optic modulator was employed driven by a high-voltage rf source. For such an electro-optic modulator, the modulation parameter is related to the half wave voltage $V_{\lambda/2}$ and peak applied rf voltage V_p by

$$\theta_m = \frac{\pi}{2}\frac{V_p}{V_{\lambda/2}}. \tag{2}$$

A 60 MHz driver was constructed using an uhf tetrode tube, Fig. 2, which applied a 200-μs-long pulse of 6 kV peak-to-peak rf voltage onto the electro-optic crystal.

Two electro-optic modulators were used in the present study. The first employed the longitudinal Pockels effect in a 12-mm diam cylindrical KD*P crystal 24 mm long with two 8-mm-wide cylindrical end electrodes.[25] The crystal was held in a refractive index matching

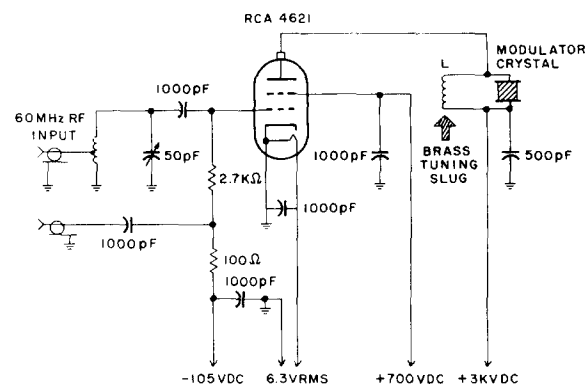

FIG. 2. Circuit diagram of the high voltage 60-MHz tetrode modulator driver.

liquid cell with Brewster-angled windows. The half-wave voltage of the cell at 1.06 μm was $V_{\lambda/2} = 6.8$ kV, and with 3 kV peak rf voltage, loss modulation of up to 41% could be obtained. The corresponding modulation parameter was $\theta_m = 0.69$.

The second modulator was a Brewster-angled $LiNbO_3$ crystal 40 mm long by 9 mm square cross section. The crystal was cut with the optic axis along its length and gold electrodes deposited on the x-plane side faces, in order to utilize the transverse Pockels effect.[26] At 1.06 μm the dc half-wave voltage was $V_{\lambda/2}{}^{dc} = 1.8$ kV. Extrapolating from measurements at 0.6328 μm[27,28] the high-frequency half-wave voltage was approximately 1.5 times the dc half wave voltage, due to the large piezoelectric contribution. Thus the high-frequency half-wave voltage was estimated as $V_{\lambda/2}{}^{ac} = 2.7$ kV and the maximum depth of modulation with the 3 kV peak driver corresponds to a modulation parameter of $\theta_m = 1.75$. It was noted that more care was required in utilizing the $LiNbO_3$ crystal than the KD*P. The $LiNbO_3$ sample used was subject to birefringence induced by mechanical stresses and thermal gradients. Because of its dispersion and high index of refraction there is 3.3° angular difference in the alignment of the Brewster-angled crystal between 0.6328 and 1.06 μm. The crystal side faces were ground to minimize acoustic resonances at 60 MHz. Finally, the $LiNbO_3$ crystal was used very close to its optical damage threshold. Similar crystals, with antireflection coated perpendicular end faces or 3° angled end faces were unable to withstand the strong optical field, and after several shots surface damage was observed. However the Brewster-angled crystal has withstood several thousand shots and is still in operation.

An important factor in the use of an active modulator is the frequency stability and harmonic distortion of the rf electrical signal. An estimate of the frequency stability requirement for the present system can be made by requiring that during the build-up time of ~400 round trips the circulating optical pulse and the rf modulation remain synchronized to within 100 ps, approximately the duration of the final pulse. This corresponds to a frequency stability of $\pm 3 \times 10^{-5}$ or ± 2 kHz at 60 MHz. In practice a change of ± 10 kHz in drive frequency leads to a noticeable increase in output pulse width and an increase in the lasing threshold. The same stability requirement holds for the laser cavity length, and considering the linear coefficient of expansion of the steel and aluminum mounting frame of $(1-2) \times 10^{-5}\,K^{-1}$, a temperature stability of ± 1 K was necessary. In addition, if the rf driver stages were improperly tuned and the final rf signal was distorted so that the positive and negative voltage swing periods were unequal, the output pulse length increased accordingly.

C. Q-Control

In conventional actively Q-switched lasers the gain is very high when the optical gate is opened and the buildup time is short, typically less than 1 μs. When an active modelocking element is incorporated in the system the final pulsewidth, in the transient buildup regime, is proportional to $M^{-1/2}$, where M is the number of passes through the modulator.[14] Thus, in order to produce short pulses a long buildup time is necessary. One way to accomplish this is to employ a partial Q-step which allows a small net gain in the cavity giving a slow pulse buildup lasting several microseconds. A full Q-step is then applied before the pulse reaches its peak to permit the pulse to quickly build up to its maximum value.[13,15,29] In the present case the operations of Q-control and final pulse switchout from the cavity were accomplished with the aid of a single, three-electrode, cylindrical KD*P Pockels crystal. The 24-mm-long, 8-mm-diam crystal was coated with three cylindrical gold electrodes, each 5 mm wide, as shown in Fig. 3(a). One half the crystal was used for Q-control and the other half was used for pulse switchout with the center electrode being a common ground.

The basic Q-step used to extend the build-up time is shown in Fig. 3(b). During optical pumping of the laser rod a half-wave voltage of $V_0 \sim 6.8$ kV was applied to the Pockels crystal to allow gain buildup. Then at time t_1, when the gain reached its maximum, the Pockels crystal voltage was reduced to a voltage V_1 permitting a small round trip net gain for the laser pulse. After several microseconds, at time t_2, the voltage is dropped to zero to allow the pulse to quickly build up to its maximum value. At this time a half-wave voltage can be applied to the second half of the Pockels crystal, Fig. 3(b), in order to switch the pulse out of the cavity. By controlling the partial Q-step voltage, V_1, the length of time that it is applied, and the level of optical pumping, the pulse buildup time can be adjusted to whatever is desired. The electrical voltages necessary were generated by employing E.G.&G. KN-22 Krytrons in the circuit shown in Fig. 3(c).

As noted previously by other workers,[27,28] the optical transmission of such a Pockels crystal, unfortunately does not exactly follow the applied electrical voltages on a microsecond time scale. The strain in the crystal due to the piezoelectric effect of the half-wave voltage relaxes on an acoustic time scale of a few microseconds, and the total birefringence is altered during this time due to the elasto-optic effect. The amount of this effect is just the difference between the high frequency and dc values of the electro-optic coefficient. Measurements of the optical transmission made at 1.06 μm indicated a ringing variation in the transmission which reaches a maximum ~3.5 μs after the Q-step and every 5 μs thereafter. Because of this effect, the optimum output time of the system was ~3.5 μs after t_1, and the duration of the partial step $(t_2 - t_1)$ was usually set around 2 μs.

It was also observed that the use of the Q-step improved the mode quality of the output relative to that of the laser operating in the free running regime. This is attributed to the fact that during the partial Q-step there is a slightly lower field on axis in the Pockels crystal than at the edges, and thus the transmission at the center

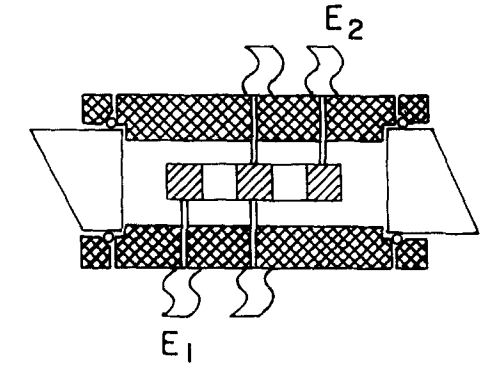

(a)

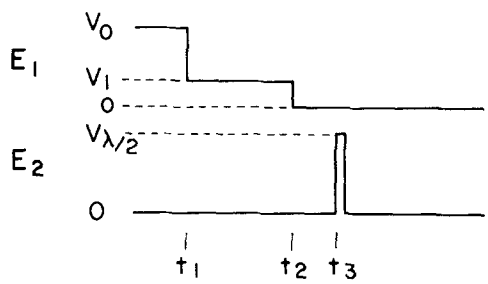

(b)

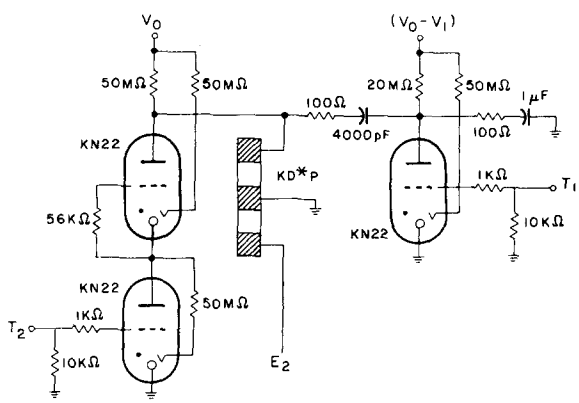

(c)

FIG. 3. (a) Cross-sectional view of the three electrode Q-control and switch-out Pockels cell showing the cylindrical three-electrode KD*P crystal in a sealed index-matching liquid housing with O-ring sealed Brewster-angled end windows. (b) The voltages E_1 applied for the standard Q-control step and E_2 applied for pulse switch-out. (c) Circuit diagram of the Krytron circuit used to generate the above Q-control voltage.

is higher. This soft aperture effect would favour the lowest order transverse mode over higher orders giving good mode quality output.

D. Pulse switch out

There are a number of output options in the present laser system. Approximately 3% of the cavity radiation is reflected off of each of the dielectric polarizers due to natural and induced birefringence in the laser system. Normally the pulse travelling in the counter-clockwise (CCW) direction was used. The train of pulses reflected off the dielectric polarizer, PL_1, was usually used for diagnostic purposes, i.e., pulse buildup time monitoring and self-triggered switch out. When an output train was desired the train reflected off the dielectric polarizer PL_2 was used.

The single circulating pulse in the ring resonator could be extracted from the cavity by applying a fast half wave voltage pulse to the switch-out Pockels crystal. The full pulse would then be reflected off the dielectric polarizer PL_2 the next time it passed through the Pockels cell. This switch out pulse could be generated at any point of the laser train with the aid of a laser-triggered spark gap in the train monitor beam, or could be generated externally to synchronize the single pulse with an external event.

II. SYSTEM PERFORMANCE

A. Reproducibility

The output pulse train reflected off the polarizer PL_1, was monitored every shot by a silicon photodiode together with a voltage monitor of the Q-step, displayed on an oscilloscope as shown in Fig. 4(a). This permitted

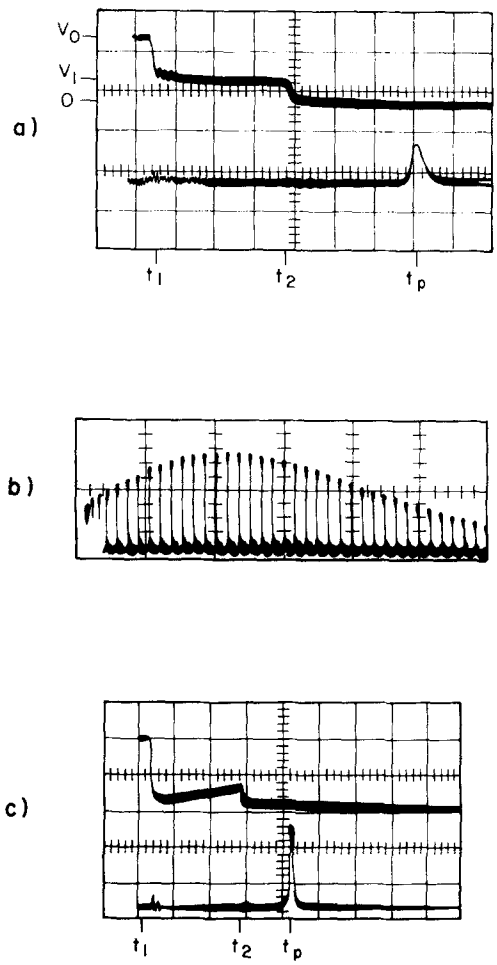

FIG. 4. (a) Oscilloscope picture of the Q-control voltage (upper trace) and monitor photodiode signal (lower trace) at 500 ns/div. (b) Oscillogram of the output train taken with a fast biplanar photodiode and Tektronix 519 oscilloscope at 50 ns/div. (c) Oscilloscope picture of an increasing partial Q-step and the corresponding monitor photodiode signal at 1 μs/div.

a measurement of the buildup time, τ_B, from the first Q-step to the peak of the laser pulse. The output train from polarizer PL_2 was measured using a fast biplanar photodiode and a Tektronix 519 oscilloscope giving pulse trains as shown in Fig. 4(b). The output consisted of a train of resolution limited pulses (<600 ps), separated by the 8.3 ns round-trip time, the train itself having a duration of ~200 ns (FWHM). The laser was fired automatically every 60 s to ensure stable operation. Using the KD*P modulator measurements were made of the peak intensity of the laser train for 40 successive shots which are plotted in histogram form in Fig. 5(a). The resulting standard deviation in the peak amplitude was ±11%. The buildup time, τ_B, was also measured for 26 shots under the same conditions, Fig. 5(b), indicating a jitter in the appearance time of the output train of ±60 ns.

B. Single pulse output

When the laser cavity was dumped by the switch-out Pockels cell, a single pulse with an energy of up to 1.5 mJ could be extracted. With a saturable dye cell of ~2% small signal transmission inserted in the output beam, a single pulse to background intensity ratio of 10^3 was obtained.

The pulse duration was measured with the aid of an S1 picosecond streak camera based on an RCA 73435C shutter tube with deflection voltages provided by an independent laser-triggered spark gap or avalanche transistor circuits triggered by a photodiode. The latter system proved to be very reliable giving streak photographs ~90% of the time with a system resolution of ~13 ps. Using a 2 μs duration partial Q-step with 70% transmission and a total buildup time of 3.3 μs the output laser pulse temporal profile was studied as a function of the depth of modulation. Using the KD*P modulator the pulse duration changed from 1.3 ns to ~200 ps as θ_m was changed from 0.2 to 0.7. Using the $LiNbO_3$ modulator to depths of modulation $\theta_m = 1.7$ a pulsewidth of ~100 ps were obtained. These results are shown in Fig. 6. For both devices lower depths of modulation produced poor results due to residual birefringence. For comparison the simple theory for the transient buildup of mode-locked pulses[14] predicted a pulse duration [FWHM] of

$$\tau_p = \frac{1}{\pi\theta_m f_m}\left(\frac{\ln 2}{M}\right)^{1/2}, \tag{3}$$

where M is number of round trips during the pulse buildup. This predicted pulse duration is plotted as a solid line in Fig. 6 for the case where $M = 400$ (i.e., $\tau_B = 3.3$ μs) and $f_m = 60$ MHz. It can be seen that there is reasonable agreement between the measured pulse duration and that predicted by Eq. (3) except at lower depths of modulation where residual birefringence becomes an important factor.

Streak photographs, Fig. 7, of the laser pulse with the KD*P modulator and $\theta_m = 0.7$ show considerable substructure, typical of the originally spiky noise structure from which the pulse grew. Over many shots some regularity could be observed in the substructure which could possibly be related to weak etalon effects between the square ends of the crystals and the quartz windows of the Pockels cells which were filled with a liquid of refractive index $n \simeq 1.2$. The corresponding spectral width of these pulses was ~4 Å (FWHM) which would be compatible with 8 ps duration substructure in the

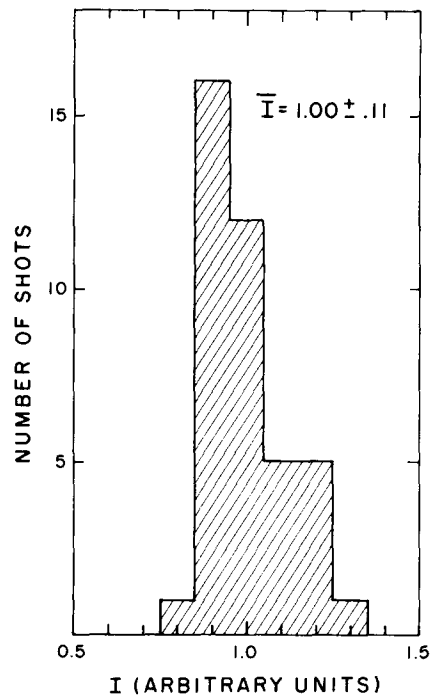

(a)

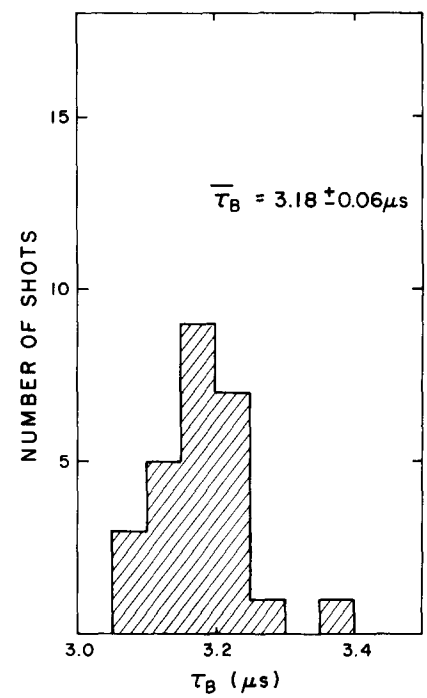

(b)

FIG. 5. (a) Histogram of the peak output train intensity I (arbitrary units) for 40 successive laser shots. (b) Histogram of the buildup time $\tau_B = t_p - t_1$ for 26 laser shots.

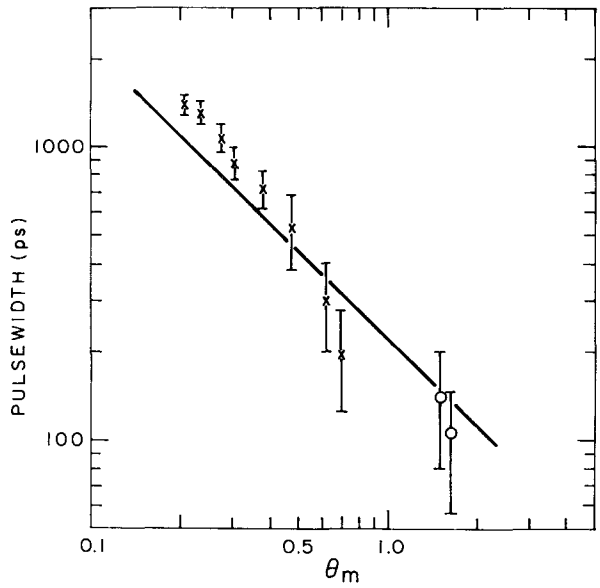

FIG. 6. Plot of the output pulsewidth versus the depth of modulation for normal Q-control operation: × —data using KD*P modulator; ○— data from the $LiNbO_3$ modulator. The predicted pulse width for f_m = 60 MHz and M = 400 is graphed as a solid line.

pulse. It would be possible to eliminate such substructure by introducing narrow bandwidth tuning etalons in the laser cavity.

C. Prelase pulse shortening

From active mode-locking theory[11,14] it is known that long build-up times of the order of a hundred microseconds are necessary to reach a steady-state value of pulse duration. This steady-state pulse duration is given by[14]

$$\tau_p^0 = \frac{\sqrt{2\ln 2}}{\pi} \frac{g^{1/4}}{\theta_m^{1/2}} \left(\frac{1}{f_m \Delta f}\right)^{1/2}, \tag{4}$$

which, for a gain bandwidth of $\Delta f = 2.67 \times 10^{12}$ s^{-1} ($\Delta\lambda \sim 100$ Å), single-pass laser medium gain $g = 0.3$, and $\theta_m = 1.74$, gives a limiting steady state pulse duration of 17 ps. Thus, simple buildup time-extending schemes as utilized in the present study still operate in a transient pulse shortening regime where the final pulse duration is proportional to $M^{-1/2}$. This limitation can be circumvented by permitting some prelase in the laser cavity for a long period of time in order to establish a short starting pulse of very weak intensity before the main Q-switch.[4] Such prelase was introduced in the present system by the employment of a simple leaky Q-switch. That is, a Q-control voltage of 1.3 kV, corresponding to 9% optical loss, was used up to time t_1 with full transmission thereafter. The rf modulation was turned on ~110 μs before the Q-switch and the flashlamp pumping was set at a level sufficient to provide some weak prelasing during this period. After time t_1 the pulse built up several orders of magnitude in intensity and was switched out of the cavity. The dependence of pulse duration on the modulation parameter θ_m is shown in Fig. 8, where it can be seen that pulses as short as 37 ps can be generated at the maximum depth of modulation. Since the prelase intensity level in this regime is not well controlled, a large jitter (±0.8 μs) is observed in the total buildup time.

D. Saturable dye pulse shortening

Another approach to further shortening the pulse is to incorporate a saturable dye into the laser cavity working together with the active modulator.[16,30,31] This

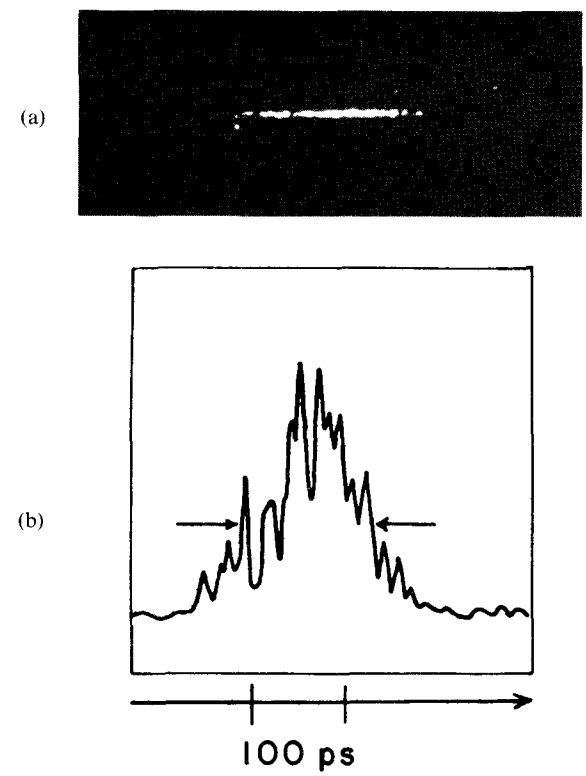

FIG. 7. Streak picture (a) and corresponding densitogram (b) of the output laser pulse for θ_m = 0.69 using the KD*P modulator. The arrows indicate the full width at half maximum intensity.

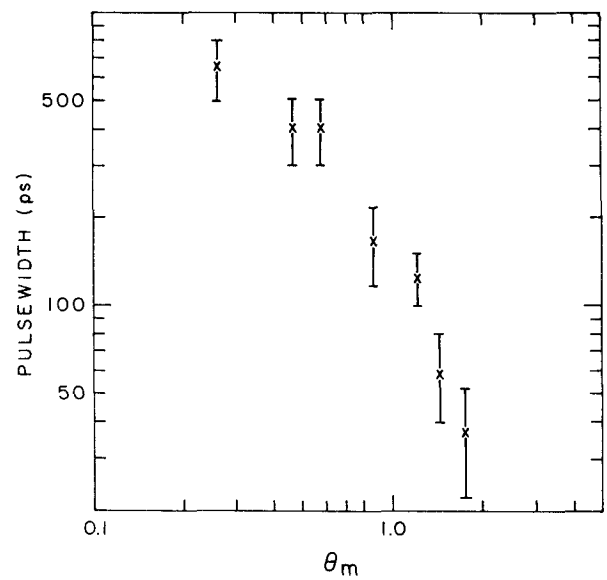

FIG. 8. Plot of the pulsewidth versus the depth of modulation under prelase operation using the $LiNbO_3$ modulator.

approach was tried in the present system by inserting a saturable dye cell of Kodak 9740, having a small signal transmission of 70%–80%, at the position of M_2 in the resonator. Only the KD*P modulator was employed at maximum depth of modulation because of the risk of damaging the $LiNbO_3$ with the higher laser intensities. The partial Q-step was reduced so that the combined loss of the dye cell and initial Q-step were on the order of 30%–35%. It was possible[16] to generate pulses of duration down to 15 ps but only in cases where a longer buildup time of 5 to 10 μs was allowed with a large increase in the jitter in the build-up time. As noted previously by the present authors[16] the combination of active and passive mode-locking produces much more reproducible output from shot to shot, with no satellite pulse trains, than does passive modelocking alone.

It is well known that the discrimination and pulse shortening effects of a saturable absorber are effective only over a limited range of pulse intensities, in this case in the range of 1 to 50 MW/cm^2. The effectiveness of the dye depends on how many times the pulse passes through the dye cell in this range of intensities and hence long buildup times with many passes are necessary for effective modelocking. If the pulse development can be controlled to allow fast build-up to this effective intensity level and then slow build-up in this range of intensities before saturating the dye, a much faster overall buildup time could be achieved without sacrificing the effectiveness of the dye. This can be accomplished by employing a Q-step as illustrated in Fig. 4(c), where the voltage is initially dropped to zero at time t_1 and then increased at a rate of ~680 V $(\mu s)^{-1}$ until a time t_2, when it is again switched to zero. Simple two-pulse computer simulations similar to those in Ref. 17 indicate substantial discrimination effects are obtained if the laser pulse just reaches an intensity ~15 MW/cm^2 and starts to lose intensity before the end of such a Q-step. Under these conditions the output pulse should appear from 100 to 200 ns after t_2. Actual pulse measurements made under such operating conditions with $t_2 - t_1 = 2.5$ μs, $\tau_B \simeq 2.7$ μs, and a dye cell solution with a small signal transmission of 75% showed only a minor improvement over the normal double Q-step operation for such short buildup times. This may be due in part to the acousto-optic birefringence effects, previously noted in the KD*P crystal, counteracting the rising voltage step.

E. Unidirectional travelling wave

The use of a dye cell for pulse shortening led to the idea of also using it to provide travelling wave operation of the ring laser.[17] This is possible since at the position of the dye cell, the counter-clockwise (CCW) propagating pulse exiting from the rod is at its maximum intensity on its trip around the ring cavity, while the clockwise (CW) propagating pulse is at its minimum intensity having suffered all the losses in the system. By placing a saturable absorber at this point the CCW pulse saturates the dye first, gains preferentially over the CW pulse, and depletes the gain of the rod before the CW pulse has a chance to grow to its full value. This method is applicable only when there is a stronger modelocking element in the laser cavity which forces the counter-propagating pulses to meet in that element, so that they do not meet in the saturable-dye cell. As with passive mode-locking the longer the build-up time the more effective is the discrimination between pulse directions. Measurements were made using a solution of Kodak 9740 dye in chlorobenzene with an initial small signal transmission of 0.7, and a 1.8 μs partial Q-step giving a transmission of ~0.84 in the KD*P modulator. Discrimination ratios of 5–75 times between the counter-propagating directions were obtained for total buildup times from 3.4 to 5 μs. These results are in qualitative agreement with the predictions of pulse buildup from the two pulse computer simulations.[17]

III. SYNCHRONIZABILITY

The main purpose of developing the laser system was to provide an ultrashort 1.06 μm laser pulse which could be synchronized to an external event. The jitter in the pulse build-up time is ~±60 ns, which is less than its 200 ns (FWHM) lifetime in the laser cavity. Thus there is a high probability that the output pulse train could be synchronized to some experiments such as the gain measurements of a XeF laser discharge[20] with the 3rd harmonic of the laser output. In this case the XeF amplifier was triggered electrically at a preset delay relative to the Q-switch of the Nd : glass laser so that its short-gain life-time would appear at some time as the train of third harmonic pulses was passing through the discharge. The combined jitter of both laser systems led to a synchronization success rate of ~75%.

The next level of synchronization required switching out the pulse from the Nd : glass laser system by means of an external trigger signal. As long as this external signal is fixed in time relative to the Q-step one can guarantee an output pulse which has an amplitude of 50%–100% of its peak value within 8.3 ns of this external trigger. Complete synchronization requires that the external event be locked in phase relative to the 60 MHz rf modulating frequency of the Nd : glass laser so that the time that the 1.06 μm pulse passes through the output polarizer is fixed relative to the external event. The switch-out crystal can then be activated within the correct 8.3 ns period to allow the 1.06 μm pulse out of the ring cavity.

As an example the scheme that was used to produce a 1.06 μm laser pulse exactly synchronized to a single 1 ns 10.6 μm CO_2 laser pulse is shown in Fig. 9. In this case it was necessary to generate a 0.53 μm optical probe pulse to study the plasmas produced off solid targets by the greatly amplified nanosecond CO_2 pulse.[19] The main discharge of the CO_2 laser and the Q-switch of the ring laser were triggered at the proper times to permit the pulse intensities to reach their peak values in both resonators at approximately the same time. During

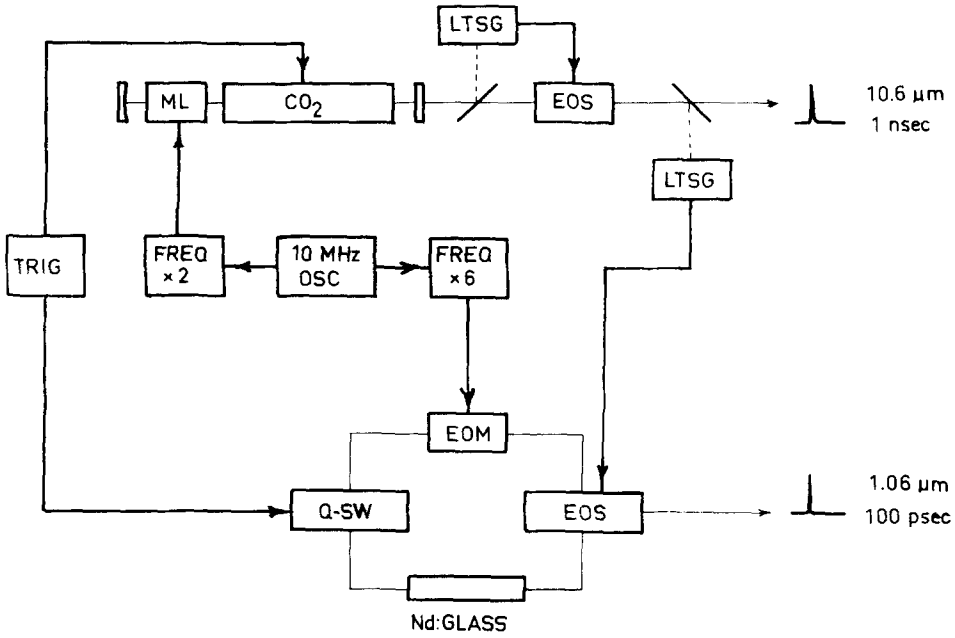

FIG. 9. Schematic diagram of the scheme used to synchronise a single 10.6-μm CO_2 laser pulse and the single 1.06-μm Nd:glass laser pulse. CO_2–CO_2 laser discharge; EOM—electro-optic modulator; EOS—electro-optic switch; LTSG—laser-triggered spark gap; ML—acousto-optic mode-locker for 10.6 μm; Q-SW—Q-control of the ND:glass laser.

the pulse buildup the 20-MHz acousto-optic modulator in the CO_2 laser and the 60-MHz electro-optic modulator in the ring laser were driven from a common 10-MHz oscillator, ensuring that the pulses in both cavities were locked in phase. A single CO_2 laser pulse was selected by an electro-optic gate. Part of this pulse actuated a laser-triggered spark gap producing an electrical pulse which switched out the 1.06 μm pulse from the ring cavity. The synchronization of the two laser pulses was measured to be better than 400 ps, the measurement resolution limit, for numerous successive shots. This synchronization scheme has resulted in the reliable production of a diagnostic probe pulse for use in studying CO_2 laser-plasma interactions.

The authors wish to acknowledge the technical expertise of W. J. Orr in designing and constructing the modulator and Q-control circuitry, the continuing technical support of P. Burtyn and G. Berry and the NRC Optical Component Laboratory for the fabrication of many optical components.

[a] Present address: University of Sofia, Sofia, Bulgaria.
[b] Present address: University of Toronto, Toronto, Canada.

[1] A. J. DeMaria, D. A. Stetser, and H. Heynav. Appl. Phys. Lett. **8,** 174 (1966).
[2] R. G. Greenhow and A. J. Schmidt, Adv. Quantum Electron. **2,** 157 (1974).
[3] W. H. Lowdermilk and J. E. Murray, IEEE J. Quant. Elec. **QE-13,** 66D, paper 14.2 (1977).
[4] D. J. Kuizenga, IEEE J. Quant. Elect. **QE-13,** 66D, paper 14.3 (1977); Opt. Commun. **22,** 156 (1977).
[5] M. C. Richardson, N. H. Burnett, H. A. Baldis, G. D. Enright, R. Fedosejevs, N. R. Isenor, and I. V. Tomov, *Laser Interaction and Related Plasma Phenomena, Vol. 4a*, edited by H. J. Schwarz and H. Hora (Plenum, New York, 1977), p. 161.
[6] V. S. Letokhov, Sov. Phys. JETP **28,** 562, 1969.
[7] P. G. Kryukov and V. S. Letokhov, IEEE J. Quant. Elect. **QE-8,** 766 (1972).
[8] A. Laubereau and W. Kaiser, Opto-electronics **6,** 1 (1974).
[9] S. E. Harris, Appl. Opt. **5,** 1639 (1966).
[10] P. W. Smith, Proc. IEEE **58,** 1342 (1970).
[11] A. E. Siegman and D. J. Kuizenga, Opto-electronics **6,** 43 (1974).
[12] C. C. Wang and L. I. Davis Jr., Appl. Phys. Lett. **19,** 167 (1971).
[13] G. V. Krivoshchekov, L. A. Kulevskii, N. G. Nikulin, V. M. Semibalamut, V. A. Smirnov, and V. V. Smirnov, Sov. Phys. JETP **37,** 1007 (1973).
[14] D. J. Kuizenga, D. W. Phillion, T. Lund, and A. E. Siegman, Opt. Commun. **9,** 221 (1973).
[15] I. V. Tomov, R. Fedosejevs, M. C. Richardson, and W. J. Orr, Appl. Phys. Lett. **29,** 193 (1976).
[16] I. V. Tomov, R. Fedosejevs, and M. C. Richardson, Appl. Phys. Lett. **30,** 164 (1977).
[17] I. V. Tomov, R. Fedosejevs, and M. C. Richardson, Opt. Commun. **21,** 327 (1977).
[18] E. D. Jones and M. A. Palmer, Opt. Quantum Electron. **7,** 520 (1975).
[19] R. Fedosejevs, I. V. Tomov, N. H. Burnett, G. D. Enright, and M. C. Richardson, Phys. Rev. Lett. **39,** 932 (1977).
[20] I. V. Tomov, R. Fedosejevs, M. C. Richardson, W. J. Sarjeant, A. J. Alcock, and K. E. Leopold, Appl. Phys. Lett. **30,** 146 (1977); I. V. Tomov, R. Fedosejevs, M. C. Richardson, W. J. Sarjeant, A. J. Alcock, and K. E. Leopold, Appl. Phys. Lett. **31,** 747 (1977).
[21] W. M. McClain, Appl. Opt. **12,** 153 (1973).
[22] J. Reader, Appl. Opt. **12,** 1405 (1973).
[23] G. Marowsky and F. Zaraga, IEEE J. Quantum Electron. **QE-10,** 832 (1974).
[24] F. C. Strome, Jr., and J. P. Webb, Appl. Opt. **10,** 1348 (1971).
[25] L. L. Steinmetz, T. W. Pouliot, and B. C. Johnson, Appl. Opt. **12,** 1468 (1973).
[26] P. V. Lenzo, E. G. Spencer, and K. Nassau, J. Opt. Soc. Am. **56,** 633 (1966).
[27] W. D. Fountain, Appl. Opt. **10,** 972 (1971).
[28] R. P. Hilberg and W. R. Hook, Appl. Opt. **9,** 1939 (1970).
[29] D. C. Hanna, B. Luther-Davies, H. N. Rutt, and R. C. Smith, Opto-electronics **3,** 163 (1971).
[30] G. V. Krivoshchekov, N. G. Nikulin, and V. A. Smirnov, Sov. J. Quant. Electron. **5,** 1096 (1976).
[31] W. Seka and J. Bunkenburg, J. Appl. Phys. **49,** 2277 (1978).